^{27}Al(d, ^{3}He)^{26}Mg reaction at 29 MeV

J. Vernotte, G. Berrier-Ronsin, S. Fortier, E. Hourani, J. Kalifa, J. M. Maison, L. H. Rosier, and G. Rotbard
Institut de Physique Nucléaire, Boîte Postale No. 1, 91406 Orsay Cedex, France

B. H. Wildenthal
Department of Physics and Astronomy, University of New Mexico, 800 Yale NE, Albuquerque, New Mexico 87131
(Received 1 February 1993)

The ^{27}Al(d, ^{3}He)^{26}Mg reaction has been investigated at 29 MeV incident energy. Observations using a split-pole magnetic spectrograph have been made of 65 levels of ^{26}Mg in the range of excitation energy between 0 and 9.7 MeV. These levels can be identified with the known states of ^{26}Mg, which by other techniques have been assigned excitation energies with precisions of 3 keV or better. Information about the orbital angular momentum (with associated conclusions about J and π) and the single-nucleon spectroscopic factors of about 40 of these ^{26}Mg levels have been obtained through distorted-wave Born approximation (DWBA) analyses of measured angular distributions. Eight levels which are populated through the pickup of a $l_p=1$ proton have been observed at $E_x=6.878$, 7.694, 7.824, 8.050, 8.902, 9.042, 9.239, and 9.618 MeV. The two most strongly excited of these levels ($E_x=7.824$ and 9.042 MeV) were attributed in a previous study of the same reaction to the population of $1p$ hole states. The observed angular distributions of two $J^{\pi}=6^{+}$ levels are reproduced with $l_p=4$ DWBA calculations which assume g components in the ground state of ^{27}Al. The excitation energies and spectroscopic factors for positive parity states are compared with the results of a recent, complete sd-shell space, shell-model calculation. New spectroscopic information is extracted from this comparison and from the comparison of the present results with previous knowledge.

PACS number(s): 21.10.Hw, 24.10.Eq, 25.40.Hs, 27.30.+t

I. INTRODUCTION

Proton-hole states in ^{26}Mg have been investigated previously in studies of the (d, ^{3}He) reaction on ^{27}Al at 34.5 MeV [1], 52 MeV [2], and 80 MeV [3], in which levels were observed, respectively, up to 6.12, 11.3, and 5.5 MeV excitation energy. In these studies, some levels observed above $E_x\simeq 7$ MeV were attributed [2] to the creation of holes in the subshells $1p_{1/2}$ and $1p_{3/2}$. However, the identification of these $l_p=1$ levels with the complete set of known [4] states of ^{26}Mg is not possible, because of the limited energy resolution of the pickup data. A study of the ^{27}Al($e,e'p$)^{26}Mg reaction [5], in which eight levels, including those with $l_p=1$, were observed up to $E_x\simeq 11.3$ MeV did not yield more accurate values of the excitation energies.

A principal motivation of this new study of the ^{27}Al(d, ^{3}He)^{26}Mg reaction was to get an accurate value for the excitation energy of these $l_p=1$ states by taking advantage of the improved experimental energy resolution which results from using a tandem accelerator in conjunction with a split-pole magnetic spectrograph. An additional motivation was to obtain precise and complete information on experimental values of excitation energies and single-nucleon spectroscopic factors of positive-parity states in order to make a conclusive comparison with the predictions of a recent comprehensive shell-model calculation for sd-shell nuclei.

II. EXPERIMENTAL PROCEDURE

A 29 MeV deuteron beam from the upgraded Orsay MP Tandem Van de Graaff accelerator was focused onto a target placed at the center of a scattering chamber, with the beam then being stopped in a graphite Faraday cup connected to a current integrator. The self-supporting target was prepared by *in vacuo* evaporation of aluminum metal. The number of aluminum nuclei in the target ($\mathcal{N}=8.63\times 10^{17}$ nuclei cm^{-2}) was determined with an accuracy of about 6% by measuring the elastic scattering of 29 MeV deuterons from it at the angles $\theta_{\rm lab}=27°$, 29°, 31°, and 33°. These four angles correspond to the position of the second maximum of the elastic scattering angular distribution. The cross sections of this reaction were calculated in the optical model with the parameters of Ref. [6]. This number of aluminum nuclei corresponds to a target thickness of 39 ± 3 μg cm^{-2}.

The ^{3}He particles were momentum analyzed with an Enge split-pole magnetic spectrograph. The detection system has been described previously [7]. The signals from the detection system were stored on a magnetic tape after processing by a SOLAR 16–40 computer.

The spectrograph horizontal entrance aperture was set to $\pm 1.5°$, which leads to a solid angle $\Omega\simeq 1.6$ msr. A ^{3}He spectrum taken at $\theta_{\rm lab}=10°$ is displayed as Fig. 1. The full width at half maximum was about 16 keV for all the peaks except some ones which appear at $E_x=6.62$, 7.82,

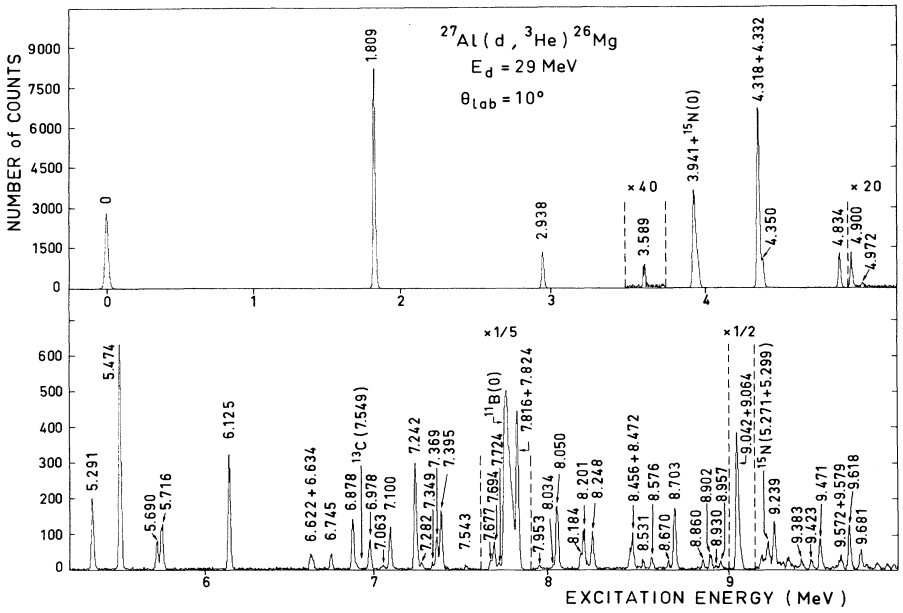

FIG. 1. Spectrum of the ^{27}Al(d,^{3}He)^{26}Mg reaction taken at $\theta_{lab}=10°$ for an accumulated charge of 1900 μC. The excitation energies are from Ref. [4]. The peaks which are due to the various contaminations are presented with the excitation energy in the corresponding final nucleus.

and 9.05 MeV. This larger width is interpreted as evidence of the contribution of several levels to the population of these peaks. In addition to the peaks which correspond to the population of levels in ^{26}Mg, there are other peaks in this spectrum which can be attributed, from their position and from their angular distribution, to the presence on the target of ^{12}C, ^{14}N, and ^{16}O contaminations.

The measured angular distributions of the ^{27}Al(d,^{3}He)^{26}Mg reaction consist of spectra taken at ten angles, ranging from 5° to 41° in the laboratory system in steps of 4°. The charge accumulated at each angle ranged from 800 μC at 5° to 2000 μC at 41°. The beam intensities in these measurements were held to within a range of 200–250 nA in order to avoid any thermal deterioration of the target; no monitor detector was employed. Constancy of the target thickness wa confirmed by taking two spectra at the same angle ($\theta_{lab}=13°$), once at the beginning and once at the end of the angular distribution measurements. These two measurements are in excellent agreement with each other.

III. ANALYSIS OF SPECTRA AND EXTRACTION OF EXCITATION ENERGIES

In order to extract the focal plane positions and integrated counts of the individual peaks in the ^{27}Al(d,^{3}He)^{26}Mg spectra, they were analyzed with the multipeak-fitting code PICOTO [8], a modified version of the code AUTOFIT [9] adapted to the VAX 85-30 computer of the Institute. Special attention was paid to verifying that the final results obtained from the computer analysis were not dependent upon the initial conditions (values of peak positions and shapes of reference peaks) which were used. The results from the analyses are thus quite reproducible except in the cases of the peaks which appear in Fig. 1 at excitation energies of about 4.33, 6.62, and 7.82 MeV. These cases will be discussed later in Sec. V.

Absolute cross sections for the reaction at each angle were obtained from the integrated counts in each peak by taking into account the integrated charge and by using the known values of the number of aluminum nuclei in the target and the spectrograph solid angle. The accuracy assigned to these cross sections is obtained by combining the uncertainties in the number of aluminum nuclei (~6%), the solid angle (~4%), and the integrated charge (~1%) with the counting statistics.

Excitation energies were determined only for peaks which were observed at three or more angles. The values were obtained from a relationship between the radius of curvature of the ^{3}He particle's trajectory in the spectrograph and the corresponding peak position in the counter. This relationship was calibrated with 12 peaks which are strongly populated at $\theta_{lab}=10°$ in the ^{31}P(d,^{3}He)^{30}Si reaction. They correspond to levels of ^{30}Si whose excitation energies are known (see Ref. [4]) with an accuracy ranging from a few hundreds of eV to, in the worst case, 2 keV. The ^{31}P(d,^{3}He)^{30}Si reaction was studied concurrently with the present experiment, in the same experimental conditions, and spectra were measured at five different values of the spectrograph magnetic field in order to calibrate the entire length of the counter. With this procedure and calibration, excitation energies in ^{26}Mg were obtained with an accuracy of ±5 keV for 65 levels (or groups of levels), ranging in excitation energy up to 9.7 MeV. These values are presented in Table I and compared there with the more complete and precise set of values from Ref. [4]. The agreement is quite good. In the remainder of this paper, the more precise values of excitation energy listed in Ref. [4] are adopted.

IV. ANALYSIS OF ANGULAR DISTRIBUTIONS

The experimentally measured angular distributions of the ^{27}Al(d,^{3}He)^{26}Mg reaction are analyzed by compar-

TABLE I. Spectroscopic information from the ^{27}Al(d,^{3}He)^{26}Mg reaction at 29 MeV.

Ref. [4]		This work				
			C^2S values			New J^π
E_x (MeV)[a]	J^π	E_x (MeV)[b]	$l=0$	$l=1$	$l=2$[c]	assignment
0	0^+	0			0.30	
1.809	2^+	1.814	0.006		1.00	
2.938	2^+	2.938	0.015		0.22	
3.589	0^+	3.590			0.006	
3.941	3^+	3.942	0.005		0.020*	
4.318	4^+	4.323	0.024		1.96	
4.332	2^+					
4.350	3^+	4.350	0.060		0.12*	
4.834	2^+	4.833	0.091		0.080	
4.900	4^+	4.898			(0.016)	
4.972±1	0^+	4.968			0.002	
5.291	2^+	5.291	0.016		0.011	
5.474±1	4^+	5.475			0.21	
5.690±1	1	5.691			0.030	1^+
5.716	4^+	5.717			0.070*	
6.125±1	3^+	6.124	0.026		0.073*	
6.256±1	0^+					
6.622±1	4^+	6.626			0.029	$(0-4)^+$
6.634±1	(0^+-4^+)					
6.745±1	2^+	6.744	0.001		0.013	
6.878	3^-	6.874		0.043		
6.978±1	5^+	6.976			0.038	
7.063±1	1^-	7.059				
7.100±1	2^+	7.099			0.059	
7.200±20	$(0,1)^+$					
7.242±1	(2^+-4^+)	7.247	0.023		0.093	$(2,3)^+$
7.261	$(2,3)^-$					
7.282	4^-	7.282				
7.349	3^-	7.350				
7.369±2	$(1,2)^+$	7.372			0.051	
7.395±1	5^+	7.397			0.085	
7.428±3	$(0,1)^+$					
7.543	$(2,3)^-$	7.543				
7.677±1	(3,4)	7.677			0.069	$(3,4)^+$
7.694±3	$(1,2^+)$	7.697		0.095		1^-
7.724±2	$(2-5)^+$	7.724			0.048	
7.773±1	$(2-4)^+$	7.771			(0.025)	
7.816±2	$(2,3)^+$	7.828			(0.07)[d]	
7.824±3	$(2,3)^-$			0.78[d]		
7.840±2	2^+					
7.851±3						
7.953±1	5^-	7.954				
8.034±2		8.030				
8.050±2	2^+	8.053		0.075		$(1-4)^-$[e]
8.184±1		8.188				
8.201±1	6^+	8.204				f
8.229±2	$(1,2^+)$	8.228				
8.248±2	1^-	8.253				g
8.399±3						
8.456±2		8.458			0.029	$(0-5)^+$[h]
8.464±2						
8.472±1	6^+	8.474				i
8.505±2		8.503				
8.531±2		8.530				
8.576±3		8.579				
8.625±1	5^-	8.626				
8.670±1	(3,5)	8.668				
8.703±1	(2^+-4^+)	8.702			0.12	$(2-4)^+$

TABLE I. (*Continued.*)

Ref. [4]		This work				
			C^2S values			New J^π
E_x (MeV)[a]	J^π	E_x (MeV)[b]	$l=0$	$l=1$	$l=2$[c]	assignment
8.860±2	2^+	8.860			(0.02)	
8.902±1		8.899		0.032		$(1-4)^-$[e]
8.930±2	(2^+-5^+)	8.930				
8.957±3		8.956				
9.020±2						
9.042±2		9.043		0.50		$(1-4)^-$[e]
9.064±1	5	9.060			(0.05)	5^+
9.111±1	6^+	9.113				
9.169±1	6^-	9.174				
9.206±2						
9.239±2	1^+	9.241		0.11		$(1-4)^-$[e]
9.261±2	4^+					
9.281±3						
9.291±2						
9.304±2						
9.317±2						
9.326±2						
9.371±2	4^+					
9.383±1	6^+	9.381				
9.423±2		9.427				
9.471±2		9.473			0.088	$(0-5)^+$[h]
9.541±1	5	9.541				
9.560±3	1^+					
9.572±2		9.576				
9.579±3	4^+					
9.590±2						
9.618±3		9.622		0.11		$(1-4)^-$[e]
9.681±2		9.683			0.045	$(0-5)^+$[h]

[a]If ΔE_x is less than 1 keV in Ref. [4], the excitation energy is rounded off to the next keV.
[b]All ±5 keV.
[c]The C^2S values of the $l_p=2$ transitions are obtained with the assumption of a $1d_{5/2}$ transfer except when the level could be identified with a shell-model level predicted to be populated through a $1d_{3/2}$ transfer (see Sec. IV). These levels are labeled with an asterisk in the table.
[d]This value of C^2S comes from the analysis of the global peak corresponding to the population of the two levels at $E_x=7.816$ and 7.824 MeV (see Sec. V C).
[e]This $J^\pi=(1-4)^-$ value corresponds to the pickup of a $l_p=1$ proton even though the presented C^2S value is obtained with the assumption of a $1p_{1/2}$ transfer.
[f]The assumption of a $1g_{9/2}$, $l_p=4$ transfer (see Sec. V D) leads to the value $C^2S=0.24$.
[g]See text, Sec. V B.
[h]This $J^\pi=(0-5)^+$ value comes from the assumption of the pickup of a $1d_{5/2}$ proton.
[i]The assumption of a $1g_{9/2}$, $l_p=4$ transfer (see Sec. V D) leads to the value $C^2S=0.15$.

isons with the results of distorted-wave Born approximation (DWBA) calculations done with the code DWUCK4 [10]. Spectroscopic factors S_{lj} are extracted from the relationship

$$\left[\frac{d\sigma(\theta)}{d\omega}\right]_{\text{expt}}=2.95\frac{C^2S_{lj}}{2j+1}\left[\frac{d\sigma_{lj}(\theta)}{d\omega}\right]_{\text{DWUCK4}}, \quad (1)$$

where 2.95 is the normalization factor for the $(d,{}^3\text{He})$ reaction [11] and S_{lj} is the spectroscopic factor for the transfer of a single nucleon of orbital angular momentum l and total angular momentum j. The isospin Clebsch-Gordan coefficient C^2 is equal to $\frac{2}{3}$ in the present case.

Since the ground state of the target nucleus in the present reaction has $J^\pi=\frac{5}{2}^+$, a single value of orbital angular momentum transfer allows several different J^π values for the state populated in the final nucleus. Specifically, $l_p=1$ transfers can lead to states of $J^\pi=(1-4)^-$ or $(2,3)^-$ in the cases of $p_{3/2}$ or $p_{1/2}$ pickup, respectively. Likewise, $l_p=2$ transfers can lead to states with $J^\pi=(0-5)^+$ or $(1-4)^+$ in the cases of $d_{5/2}$ or $d_{3/2}$ pickup, respectively. Finally, levels with $J^\pi=(2,3)^+$ can be populated through three pure or mixed transfers: $l_p=0$ ($s_{1/2}$), $l_p=2$ ($d_{5/2}$), and $l_p=2$ ($d_{3/2}$). In the present work, C^2S values are extracted under the assumption of $1d_{5/2}$ transfer for the $l_p=2$ and $0+2$ transitions, except for those final states which are identified as being populated by $1d_{3/2}$ transfer in the shell-model calculations (see Sec. V E). In the excitation energy range of the present work, the DWUCK4 cross sections are larger

for the $1d_{5/2}$ transfer (and the spectroscopic factors smaller) by a factor of 2.17, which is constant within a few percent in the angular range considered. The transfers which are considered to get the C^2S values for the $l_p=1$ transitions will be presented later in Sec. V C.

Several sets of deuteron and ^{3}He optical-model parameter sets obtained from elastic scattering studies were examined in the context of the DWBA analysis of the present ^{27}Al(d,^{3}He)^{26}Mg angular distributions. The DWBA results were critiqued in terms of how closely they reproduced the measured angular distributions of the strong, pure, $l_p=2$ transitions to the levels at $E_x=0$ and 5.474 MeV. The first transition is uniquely $d_{5/2}$, because the ground state of ^{26}Mg has $J^\pi=0^+$. The second transition, which leads to a level with $J^\pi=4^+$, can proceed with $d_{3/2}$ as well as $d_{5/2}$, as indicated above. However, the analyses were carried out with the assumption of pure $j=\frac{5}{2}$ transfer, since such a transfer is predicted for this level by the shell-model calculations.

Three deuteron optical parameter sets were used to generate the DWBA predictions for these two "test" transitions. They are adapted for ^{27}Al from relationships obtained in the analyses of deuteron elastic scattering on many nuclei. The first deuteron parameter set [12] is obtained from the analysis of the elastic scattering of 34 MeV deuterons by a number of light and medium nuclei, which, however, included only ^{16}O and ^{40}Ca from the *sd* shell. Optical-model parameter sets generated from the relationships of Ref. [12] have been used in the analysis of much transfer-reaction data (see Ref. [1] for instance). The second parameter set [13] is obtained from a global analysis of vector analyzing power data for 52 MeV elastic scattering of polarized deuterons on nine nuclei, including five *sd*-shell nuclei, in conjunction with previous elastic scattering measurements done at the same energy [14] for 27 nuclei (including eight *sd*-shell nuclei). The optical-model parameter sets obtained from Ref. [14] have been used in studies of the (d,^{3}He) reaction on a number of *sd*-shell nuclei (see, for instance, Ref. [15] and references therein). The third parameter set is adapted from the relationships (L potential) which are presented in Ref. [6]. These relationships (which include a dependence upon the deuteron energy) are from a global analysis of a large number of elastic scattering and polarization data obtained in various studies (including Ref. [14]) at various deuteron energies ranging from 12 to 90 MeV.

Each of these three deuteron parameter sets was combined with four different ^{3}He optical parameter sets to generate the test DWBA comparisons. The ^{3}He sets were deduced from the analysis [16] of 25 MeV ^{3}He elastic scattering from ^{26}Mg. These sets are characterized by either a volume or a surface imaginary part and by real depths of about 150 MeV ("medium" family) or 200 MeV ("deep" family). The elastic scattering data in the angular range $\theta_{lab}=12°-90°$ are accounted for quite well by each of these four sets of parameters. For all the combinations of deuteron and ^{3}He optical parameter sets, the proton bound-state form factor used in the DWBA calculations is generated with a standard Woods-Saxon well, the depth of which is adjusted to reproduce the experimental proton separation energy.

The cross sections resulting from the local and zero-range DWBA calculations done with these 12 combinations of deuteron and ^{3}He optical parameter sets are in a correct agreement with the experimental data. Especially, the first maximum of the experimental angular distributions is quite well accounted for. The mean value of the 12 C^2S values was calculated for each of the 2 $l_p=2$ transitions. The deviation between the individual C^2S values and the mean value is less than 10%. These 12 combinations lead also to very similar shapes for the $l_p=1$ transitions. As a consequence, the strong transition to the level at $E_x=9.042$ MeV, the experimental angular distribution of which is quite well accounted for by these $l_p=1$ DWBA calculations, was also considered as a third "test" transition. In this case also the deviation between the individual C^2S values and the mean value is less than 10%.

The following analysis was done with the deuteron potential of Ref. [6] and with the ^{3}He potential of the "deep" family with a volume absorption. A reason for this choice is that deuteron and ^{3}He optical parameter sets with the same origin were previously used in the analysis of the ^{30}Si(^{3}He,d)^{31}P reaction at 25 MeV [7]. The various optical parameter sets (deuteron, ^{3}He, and transferred particle) are presented in Table II.

DWBA calculations including finite-range and nonlocality corrections were also done for the three "test" transitions. The nonlocal parameters for ^{3}He, deuteron, and proton were 0.25, 0.54, and 0.85 fm, respectively. The finite-range parameter was 0.77 fm [11]. These calculations result in a reduction by 25–30 % of the spectroscopic factors and a slightly worse fit to the experimental points as it can be seen in Fig. 2. The remainder of the analysis was done without these corrections.

The experimental angular distributions are presented along with the DWUCK4 predictions in Figs. 3 and 4 for the $l_p=1$ and 2 transitions, respectively, and the C^2S values are given in Table I. These C^2S values are ob-

TABLE II. Optical-model parameters used in DWBA calculations.

Channel	V (MeV)	r_r (fm)	a_r (fm)	W_V (MeV)	$4W_D$ (MeV)	r_i (fm)	a_i (fm)	$V_{s.o}$ (MeV)	$r_{s.o}$ (fm)	$a_{s.o}$ (fm)	r_c (fm)
^{27}Al+d	84.8	1.17	0.758	1.1	47.6	1.325	0.740	6.49	1.07	0.66	1.30
^{26}Mg+^{3}He	217.6	1.15	0.636	32.5		1.319	0.986				1.40
Proton	a	1.25	0.65					$\lambda=25$	1.25	0.65	1.25

[a]The depth is adjusted by the code DWUCK4.

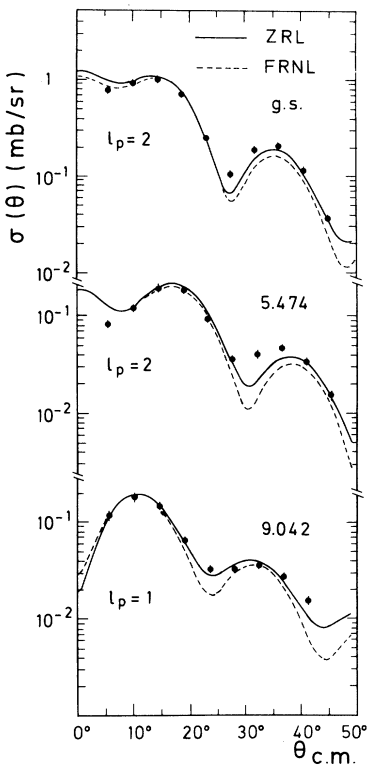

FIG. 2. Angular distributions from the ^{27}Al(d,^{3}He)^{26}Mg reaction leading to the levels at $E_x = 0$, 5.474, and 9.042 MeV. Curves result from DWBA calculations done for the indicated l_p values in the zero-range, local approximation (ZRL, solid curves) and in the finite-range, nonlocal approximation (FRNL, dashed curves).

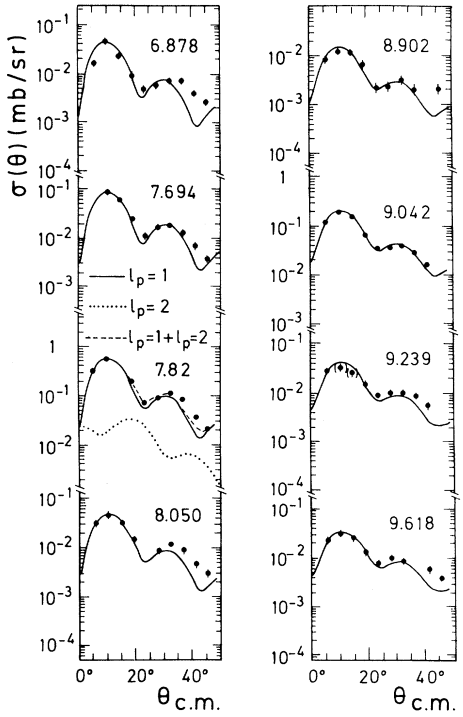

FIG. 3. Angular distributions from the ^{27}Al(d,^{3}He)^{26}Mg reaction leading to odd-parity levels. If not shown, the error is less than the point size. Curves result from DWBA calculations done for $l_p = 1$ transitions. For the $E_x = 7.82$ MeV case, the experimental data are due to the excitation of two levels at $E_x = 7.816$ and 7.824 MeV, $l_p = 2$ and 1, respectively, which could not be resolved in this work. The DWBA analysis of these data was done as described in Sec. V C. The solid and dotted curves are the DWBA predictions for $l_p = 1$ and 2, respectively. The dashed curve is the sum of the $l_p = 1$ and 2 contributions weighted by the C^2S values of Table I. As to the experimental points between parentheses for the $E_x = 9.239$ MeV level, see Sec. V B.

tained by trying to reproduce at least the first maximum of the experimental angular distributions. It can be seen in Fig. 4 that the quality of the agreement between the shapes of the experimental and DWUCK4 cross sections for the $l_p = 2$ transitions is nice enough in the first MeV of excitation energy (except for the level at $E_x = 4.900$ MeV), but becomes less good at higher excitation energies. A tentative explanation is that the incident deuteron energy of the present work is not high enough to warrant an equally safe DWBA analysis in the whole 0–10 MeV excitation energy range. For the $l_p = 2$ transfer the value of the DWUCK4 cross section at the first maximum is continuously decreasing from 7.2 to 0.5 mb/sr in this range. For the same transfer and the same excitation energy range, a similar but smaller decrease (from 9.5 to 2.2 mb/sr) is predicted in the calculations done at 52 MeV with the optical parameters of Ref. [2] (with set B as ^{3}He set). The same behavior is observed for the $l_p = 1$ transfer in the 6.5–10 MeV excitation energy range: a decrease from 0.8 to 0.2 mb/sr at the first maximum at 29 MeV and from 1.7 to 1.0 mb/sr at 52 MeV. A larger uncertainty can be thus expected for the spectroscopic factors obtained in the present work for the higher-lying levels. However, it can be seen in Table III that there is an excellent agreement between the C^2S values obtained in the excitation energy range ($E_x < 6.2$ MeV) which is common both to this work and to previous and higher deuteron energy studies [1–3]. In a conservative way the uncertainties of the DWBA analysis are estimated to contribute a 20% systematic uncertainty to the spectroscopic factors of the most strongly populated levels; this uncertainty can be larger in the case of the weakly populated levels which have poor statistics and for which the single-step reaction model might be a poor approximation.

For some levels the J^π value of which is known [4] to be consistent with a $l_p = 2$ transfer, the population is very weak ($E_x = 8.860$ MeV, for instance) or some forward points are missing in the experimental angular distribution ($E_x = 7.773$ MeV, for instance). The C^2S values were, however, tentatively extracted for this $l_p = 2$ transfer, but they are presented in parentheses in Table I.

A $l_p = 0$ contribution was systematically investigated for all the transitions which lead to levels with $J^\pi = 2^+$ or 3^+. In the case of levels with unknown J^π values, this search was also undertaken whenever the experimental

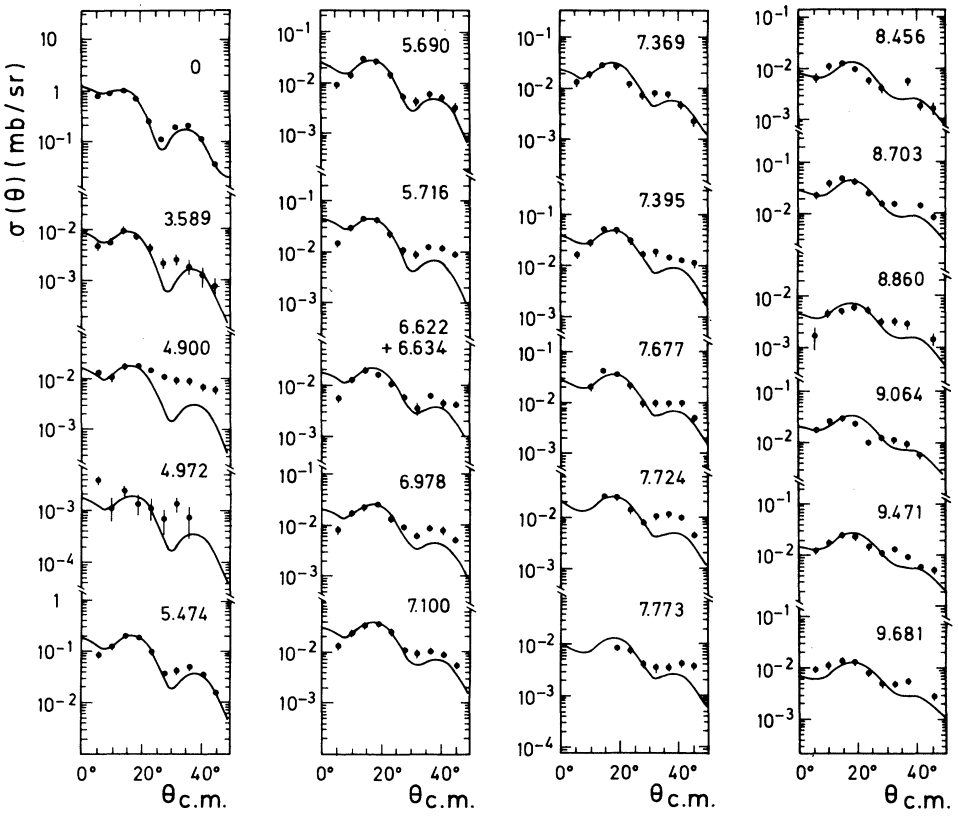

FIG. 4. Angular distributions from the ^{27}Al(d,^{3}He)^{26}Mg reaction for the $l_p=2$ transitions. If not shown, the error is less than the point size. Curves result from DWBA calculations.

TABLE III. Comparison of the C^2S values for the even-parity states.

		C^2S values					
		This work		Ref. [1][a]		Ref. [2][b]	Ref. [3][c]
E_x (MeV)	J^π	$l_p=0$	$l_p=2$	$l_p=0$	$l_p=2$	$l_p=2$	$l_p=2$
0	0^+		0.30		0.30	0.27	0.26
1.809	2^+	0.006	1.00	<0.013	1.07	0.93	0.87
2.938	2^+	0.015	0.22	<0.013	0.23	0.19	0.29
3.589	0^+		0.006		<0.013	0.013	
3.941	3^+	0.005	0.020	<0.007	<0.033	0.020	
4.318	4^+	0.024	1.96				
4.332	2^+						
4.350	3^+	0.060	0.12	<0.060	2.13	1.93	2.13
4.834	2^+	0.091	0.08	0.089	<0.160		
4.900	4^+		(0.02)				
4.972	0^+		0.002		<0.013		
5.291	2^+	0.016	0.011				
5.474	4^+		0.21		0.24	0.32	0.25
5.690	1^+		0.030				
5.716	4^+		0.070				
6.125	3^+	0.026	0.073	<0.033	0.12		

[a] $E_d=34.5$ MeV.
[b] $E_d=52$ MeV; no search was done for a $l_p=0$ contribution.
[c] $E_d=80$ MeV; no search was done for a $l_p=0$ contribution.

cross sections showed at forward angles the increase which is characteristic of the $l_p=0$ transitions. The relative strengths of the two spectroscopic factors were determined by minimizing the quantity

$$D^2=\sum_{i=1}^{N}\left[\frac{\sigma_{i,\text{expt}}-\sigma_{i,\text{DWBA}}}{\Delta\sigma_{i,\text{expt}}}\right]^2, \tag{2}$$

where $\sigma_{i,\text{DWBA}}$ stands for

$$2.95C^2S_{0+2}\left[\frac{d\sigma_i(\theta)}{d\omega}\right]_{\text{DWBA}}$$

and

$$C^2S_{0+2}\left[\frac{d\sigma(\theta)}{d\omega}\right]_{\text{DWBA}}=C^2S_{0+2}\left\{\frac{\alpha}{2}\left[\frac{d\sigma_{l=0}(\theta)}{d\omega}\right]_{\text{DWUCK4}}+\frac{1-\alpha}{2j+1}\left[\frac{d\sigma_{l=2,j}(\theta)}{d\omega}\right]_{\text{DWUCK4}}\right\}, \tag{3}$$

where α is the weight of the $l_p=0$ transition and where j can have the values $\frac{3}{2}$ or $\frac{5}{2}$. There are at least two sources of imprecision in the determination of α. The first one is that, as quoted above, the fit to the experimental data is becoming less good at higher excitation energies for the $l_p=2$ transitions. The second one is that it is not possible to check how correctly the experimental $l_p=0$ contribution is accounted for by the DWUCK4 calculations since no level is known in ^{26}Mg to be definitely populated by a unique $l_p=0$ transfer. So the assumption has been made that the $l_p=0$ experimental contribution is correctly accounted for by the DWUCK4 calculations at the five forward angles and the analysis was restricted to these five experimental data which include the first maximum of the $l_p=2$ transition. The weight α thus determined leads to the values $S_0=\alpha S_{0+2}$ and $S_2=(1-\alpha)S_{0+2}$. The experimental values of α will be compared to the shell-model ones in Sec. V E. The experimental angular distributions of these transitions are presented in Fig. 5 with the DWUCK4 predictions.

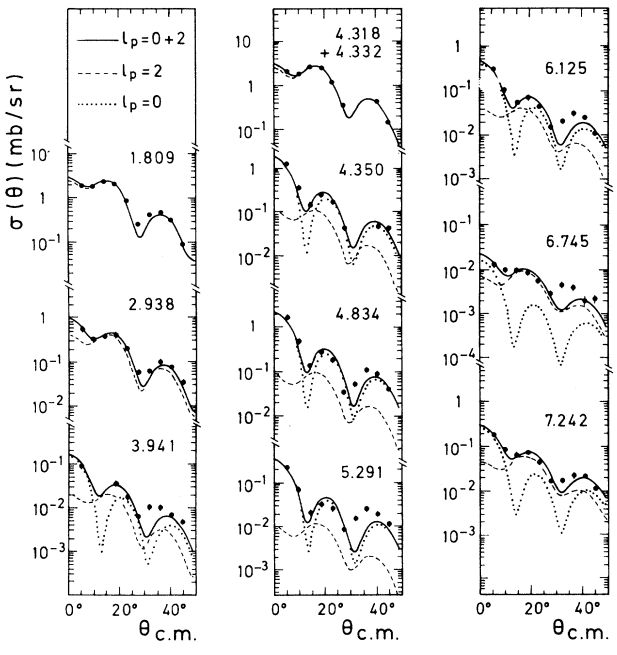

FIG. 5. Angular distributions from the ^{27}Al(d,^{3}He)^{26}Mg reaction for the $l_p=0+2$ transitions. If not shown, the error is less than the point size. Curves result from DWBA calculations. The contributions for the transitions $l_p=0$ (dotted curves) and $l_p=2$ (dashed curves), which are also displayed in this figure, are weighted by the C^2S values presented in Table I.

V. DISCUSSION

A. Triplet of levels around 4.33 MeV

The three ^{26}Mg levels at $E_x=4.318$, 4.332, and 4.350 MeV, respectively [4], could not be resolved in the previous works [1–3] in which only one peak is observed around 4.3 MeV. In the present work, two peaks are clearly apparent as can be seen in Fig. 6 which displays a part of the spectrum measured at $\theta_{\text{lab}}=9°$. The first (and most strongly populated) peak was considered as due to

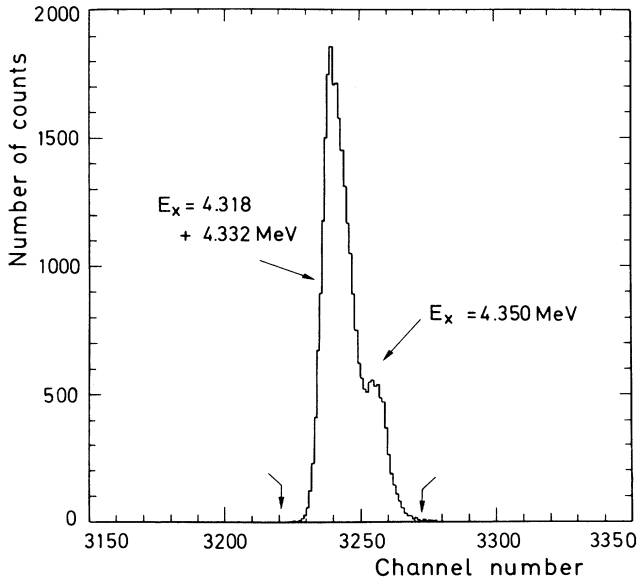

FIG. 6. Part of the spectrum of the ^{27}Al(d,^{3}He)^{26}Mg reaction at $\theta_{\text{lab}}=9°$, presenting the two peaks which are observed in the region of the triplet of levels at $E_x=4.318$, 4.332, and 4.350 MeV. The surface of the global peak is obtained by summing the number of counts between the channels indicated by arrows.

the population of the two levels at $E_x=4.318$ and 4.332 MeV. Unfortunately, it was not possible to get reliable values for the contribution of each of these two levels because the results from the code PICOTO are very dependent upon the reference peak shape and the various initial conditions of the analysis. However, at all the angles, the sum of these contributions is found to be independent upon the details of the analysis. It is also the case for the surface of the peak corresponding to the level at $E_x=4.350$ MeV. Furthermore, the summed surfaces of the three peaks are equal, within statistical errors, to the surface which is obtained by simply integrating the number of counts between two channels defining the boundaries of the global peak (as indicated by arrows in Fig. 6).

The J^π values of these three levels are 4^+, 2^+, and 3^+, respectively [4]. With the exception of the first of them, they can be populated through a $l_p=0+2$ transfer. It was therefore attempted to account for the experimental angular distributions with the superposition of pure $l_p=0$ and 2 DWUCK4 cross sections as described in Sec. IV. This analysis was done first for the summed contribution of the three levels. The best visual fit is obtained for $C^2S_0=0.10$ and $C^2S_2=2.01$, in excellent agreement with the values from Ref. [1] (Table III). However, it has to be pointed out that the visual agreement remains acceptable (with a deterioration of the fit by a factor of 2) for a change of the spectroscopic factors by 40% and 10% for the $l_p=0$ and 2 transitions, respectively. In the two other previous works, the global peak was analyzed with the assumption of a pure $l_p=2$ transition.

A similar analysis was then done for the summed contribution of the two first levels and for the contribution of the level at $E_x=4.350$ MeV (with the assumption for this level of the $1d_{3/2}$ transfer which is predicted in the shell-model calculations). The C^2S values are presented in Tables I and III. It appears that most of the $l_p=0$ transfer in this region is concentrated upon the level at $E_x=4.350$ MeV. Furthermore, if the measurement of the very small $l_p=0$ contribution ($\sim 1\%$) to the population of the main peak can be considered as significant, it definitely establishes the population of the level at $E_x=4.332$ MeV in this one-proton pickup reaction.

B. Spin and parity assignments

The J^π values which are presented in column 2 of Table I are from Ref. [4], and they represent the status of the spin and parity assignments for ^{26}Mg levels at the beginning of the present study. In most of the cases, the present results are in agreement with these assignments. In some cases, however, it was possible either to restrict the available choice for the J^π values or to make new assignments when the J^π value was unknown. Some discrepancies were also observed. All the new J^π assignments are presented in the last column of Table I and are discussed in the following.

The level at $E_x=5.690$ MeV is given $J=1$ in Ref. [4]. Positive parity is deduced for this level from the $l_p=2$ pattern of the experimental angular distribution (Fig. 4). So $J^\pi(5.690\text{ MeV})=1^+$. Similarly, positive parity is assigned to the levels at $E_x=7.677$, 8.703, and 9.064 MeV, which are also populated through $l_p=2$ transitions.

The larger experimental width of the peak at $E_x=6.62$ MeV (Sec. II) is interpreted as the evidence of the population of the two levels at $E_x=6.622$ and 6.634 MeV, $J^\pi=4^+$ and (0^+-4^+), respectively [4]. As indicated in Sec. III, it was not possible to resolve these two components with the code PICOTO. However, since the experimental angular distribution of the global peak is very similar (Fig. 4) to those of the transitions to the neighboring levels at $E_x=5.716$, 6.978, and 7.100 MeV which are all populated through $l_p=2$ transfers, it seems reasonable to assume that the two levels at $E_x=6.622$ and 6.634 MeV are populated through $l_p=2$ transfers. So the J^π values are restricted to $(0-4)^+$ for the level at $E_x=6.634$ MeV.

The experimental angular distributions of the levels at $E_x=7.242$ and 7.694 MeV are correctly accounted for by $l_p=0+2$ (Fig. 5) and $l_p=1$ (Fig. 3) transitions, respectively. The J^π values of Ref. [4], (2^+-4^+) and $(1,2^+)$, respectively, can thus be restricted to $(2,3)^+$ and 1^-, respectively, and the population of the level at $E_x=7.694$ MeV can be attributed to the pickup of a $p_{3/2}$ proton.

No J^π assignment has been done previously for the levels at $E_x=8.456$, 9.471, and 9.681 MeV or for the levels at $E_x=8.902$, 9.042, and 9.618 MeV. The present assignments, $(0-5)^+$ for the first three levels and $(1-4)^-$ for the three other ones, come from the $l_p=2$ and 1 patterns, respectively, of the experimental angular distributions.

There is a discrepancy between the J^π assignments from this work and from Ref. [4] for the level at $E_x=8.050$ MeV. The experimental angular distribution of this level, which is easily resolved in the present work from a very weakly populated level at $E_x=8.034$ MeV, exhibits a clear $l_p=1$ pattern (Fig. 3) leading to a $J^\pi=(1-4)^-$ assignment instead of 2^+ as in Ref. [4]. In this reference the $J^\pi=2^+$ assignment comes from the identification of the level at 8.050 MeV with a state at $E_x=8.045\pm0.010$ MeV which is strongly populated in the ^{24}Mg(t,p)^{26}Mg reaction [17] through a $L=2$ transition resulting from the transfer of the two neutrons in the $2p$ orbit. The discrepancy can be removed by assuming that the level which is actually populated in the (t,p) reaction is more likely the level at $E_x=8.034$ MeV. This assumption finds some support in the fact that the level at $E_x=8.034$ MeV is very weakly populated in the ^{27}Al(d,^{3}He)^{26}Mg reaction as is expected for a level with a main $(2p)^2_\nu$ configuration.

There is also a discrepancy between the J^π assignments from this work and from Ref. [4] for the level at $E_x=9.239$ MeV. In this work there was some difficulty to get the surface of the peak at the angles $\theta_{\text{lab}}=13°$ and 17° because of the presence of the contaminant peak of the ^{16}O(d,^{3}He)^{15}N(5.271+5.299 MeV) reaction. The corresponding experimental points are presented in parentheses in Fig. 3. Nevertheless, the experimental angular distribution of this level is accounted for quite correctly by a $l_p=1$ transition (Fig. 3), which leads to a $J^\pi=(1-4)^-$ assignment instead of 1^+ as in Ref. [4]. The

$J^\pi=1^+$ assignment comes from (γ,γ') and (p,p') experiments, Refs. [18] and [19], respectively. No explanation is found for this discrepancy.

At last, there is a puzzling situation with the level at $E_x=8.248$ MeV. It was not possible to account for the experimental angular distribution with pure $l_p=1$ or 2 transitions. The assumption of the population of this level through a mixed $l_p=0+2$ transition was also examined because of the shape of the experimental angular distribution at the forward angles (Fig. 7). Such a mixture would lead to the $J^\pi=(2,3)^+$ assignment in contradiction with the value $J^\pi=1^-$ of Ref. [4], which is based upon the identification of this level with a state at $E_x=8.240\pm0.010$ MeV strongly populated through a $L=1$ transition in the above-quoted (t,p) reaction [17]. However, it was not possible either to account for the experimental angular distribution satisfactorily with the superposition of $l_p=0$ and 2 transitions, as can be seen in Fig. 7. A quite equivalent fit obtained with the assumption of a proton pickup from the $1f_{7/2}$ shell is also presented in Fig. 7. Such a transfer would be in agreement with the $J^\pi=1^-$ assignment and would suggest the existence of a configuration $(f_{7/2})_\pi(f_{7/2})_\nu$ and/or $(f_{7/2})^2_\pi$ in the ground state of ^{27}Al. However, it cannot either be rejected that the state from the (t,p) reaction could correspond actually to the $J^\pi=(1,2^+)$ level at $E_x=8.229$ MeV, which would then be $J^\pi=1^-$.

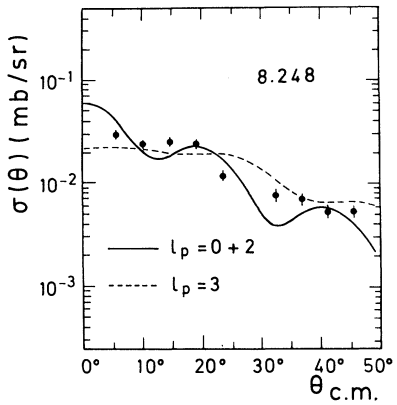

FIG. 7. Angular distributions from the ^{27}Al$(d,^3$He$)^{26}$Mg reaction leading to the level at $E_x=8.248$ MeV. The curves are from DWBA calculations done with the assumption of a $l_p=0+2$ transition with $C^2S(l_p=0)=0.007$ and $C^2S(l_p=2)=0.044$ (solid curve) and of a $l_p=3$, $1f_{7/2}$ transition with $C^2S(l_p=3)=0.023$ (dashed curve).

C. $l_p=1$ states

The states which are populated through a $l_p=1$ transfer are presented in Table IV and compared therein with those which were observed in the same excitation energy range in the previous study of the same reaction at 52 MeV [2]. These states were assigned $J^\pi=(1-4)^-$ in Table I except when more precise information about the J^π value is available from another source. The experimental angular distribution are quite correctly accounted for by the DWBA predictions (Fig. 3). The values of C^2S are obtained for the transfer which is indicated in column 2 of Table IV. It follows from the DWUCK4 calculations that the relationships

$$C^2S(1p_{3/2})\approx(0.8-0.9)C^2S(1p_{1/2})$$

and

$$C^2S(2p_{3/2})\approx(0.20-0.25)C^2S(1p_{1/2})$$

stand for all the $l_p=1$ states in the excitation energy range of this work.

On the grounds of their strong population and of their experimental angular distribution, the two peaks which are observed in this work at $E_x=7.82$ and 9.05 MeV are identified with the peaks at $E_x=7.86$ and 9.16 MeV, respectively, which are strongly excited through $l_p=1$ transitions in the study at 52 MeV. The C^2S values are 0.86 and 0.56, respectively (with the assumption of a $1p_{1/2}$ transfer). However, as indicated in Sec. II, the larger experimental width of these two peaks is interpreted as evidence of the contribution of several unresolved levels to their population, namely, the levels at $E_x=7.816$ and 7.824 MeV and at $E_x=9.042$ and 9.064 MeV for the peaks at $E_x=7.82$ and 9.05 MeV, respectively. The level at $E_x=7.816$ MeV is assigned $J^\pi=(2,3)^+$ in Ref. [4] because it is populated through a mixed $l_n=0+2$ transition

TABLE IV. Comparison of the C^2S values for the odd-parity states.

This work			Ref. [2]		
E_x (MeV)	Assumed nlj	C^2S	E_x (MeV)	Assumed nlj	C^2S
6.878	$1p_{1/2}$	0.043[a]			
7.694	$1p_{3/2}$ [b]	0.095			
7.824	$1p_{1/2}$	0.78	7.86±0.05	$1p_{1/2}$	1.76
8.050	$1p_{1/2}$	0.075			
8.902	$1p_{1/2}$	0.032	8.81±0.09	$1p_{1/2}$	≤0.30
9.042	$1p_{1/2}$	0.50	9.16±0.07	$1p_{1/2}$	1.34
9.239	$1p_{1/2}$	0.11			
9.618	$1p_{1/2}$	0.11	9.76±0.09	$1p_{1/2}$	≤0.25

[a]The value of C^2S is 0.011 if the analysis is done with the assumption of a $2p_{3/2}$ transfer.
[b]The $1p_{3/2}$ transfer is from the $J^\pi=1^-$ assignment to this level (see Sec. V B).

in the ^{25}Mg(d,p)^{26}Mg reaction [20], and the level at $E_x=9.064$ MeV is assigned $J=5$ from a study of the ^{23}Na(α,$p\gamma$)^{26}Mg reaction [21]. So the $l_p=1$ states are the levels at $E_x=7.824$ and 9.042 MeV. For the level at $E_x=7.824$ MeV, this identification is in agreement with the $J^\pi=(2,3)^-$ assignment of Ref. [4].

It was possible to resolve the components of the peak at $E_x=9.05$ MeV with the code PICOTO, and this analysis confirms that the main contribution is due to the level at $E_x=9.042$ MeV. The C^2S value of this level (Table IV) is smaller by 10% than the value 0.56 which is obtained from the analysis of the global peak. In the case of the peak at $E_x=7.82$ MeV, which could not be resolved with the peak-fitting procedure, the global experimental angular distribution was analyzed by searching for the weights of $l_p=1$ and 2 contributions as was done in Sec. IV for the $l_p=0+2$ mixed transitions. The visual fit from this analysis is better than if only a pure $l_p=1$ transition is considered. The reduction of the C^2S value for the $l_p=1$ transition (Table IV) is also 10%. The capability of the superposition method for getting reliable C^2S values was checked for cases in which the two levels could be resolved by analyzing the global experimental angular distributions obtained by adding these two contributions. For these cases (the peaks at $E_x=7.677+7.694$ MeV and $E_x=9.042+9.064$ MeV), the values of C^2S which are obtained for the various levels are identical whatever be the method used to get them.

In contrast to the case of the positive-parity states, the present C^2S values for the $l_p=1$ states are smaller than the values of Ref. [2] by at least a factor of 2. It has been pointed out, however, in Ref. [2] that the usual method of fitting the first maximum of the experimental angular distribution would lead to C^2S values smaller by about 50%–70% than those obtained by searching for the best overall fit in the whole angular range, a method which was used for the $l_p=1$ states in the study at 52 MeV.

The levels at $E_x=8.902$ and 9.618 MeV could correspond to the states previously observed [2] at 8.81±0.09 and 9.76±0.09 MeV, respectively.

The levels at $E_x=6.878$, 7.694, 8.050, and 9.239 MeV are not observed in Ref. [2]. The case of the three last levels has been previously discussed in Sec. V B. The level at $E_x=6.878$ MeV, $J^\pi=3^-$, is strongly populated through a $l_n=1+3$ mixed transfer in the ^{25}Mg(d,p)^{26}Mg reaction [20] and through a $L=3$ transfer in the ^{24}Mg(t,p)^{26}Mg reaction [17]. It is not possible to decide if the population of this state in the present work comes from the pickup of a proton from the $1p$ or $2p$ shells. In this case it would establish the presence of a configuration $(2p_{3/2})_\pi(2p_{3/2})_\nu$ and/or $(2p_{3/2})^2_\pi$ in the ground state of ^{27}Al. The C^2S value of Table IV is extracted with the assumption of a $1p_{1/2}$ transfer.

The state which is observed at 11.32±0.13 MeV in Refs. [4] and [5] is out of the excitation energy range investigated in the present work.

For the $1p_{1/2}$ transitions, the C^2S values of Table IV add to 1.64. This indicates that about 80% of the $1p_{1/2}$ strength is observed in the present work, if all the transitions are actually $1p_{1/2}$.

D. Levels at $E_x=8.201$ and 8.472 MeV

The shapes of the experimental angular distributions of the two levels at $E_x=8.201$ and 8.472 MeV are very similar and structureless as can be seen in Fig. 8. These levels were assigned $J^\pi=6^+$ from γ-decay scheme, lifetime, and proton–γ-ray angular correlation measurements obtained in a study of the ^{23}Na(α,$p\gamma$)^{26}Mg reaction [21]. The population of these levels through a direct one-step reaction mechanism would imply a $l_p=4$ transfer and therefore the presence of a g component in the ground state of ^{27}Al. Such DWUCK4 calculations lead to a reasonable fit to the experimental data (Fig. 8). The values of C^2S which are obtained with the assumption of a $1g_{9/2}$ proton pickup are 0.24 and 0.15 for the levels at $E_x=8.201$ and 8.472 MeV, respectively.

Another example of a possible $l_p=4$ proton pickup in the sd shell can be found in the population of the ^{27}Al level at $E_x=3.004$ MeV, $J^\pi=\frac{9}{2}^+$, in the ^{28}Si(d,^{3}He)^{27}Al reaction [15,22,23] even though there is no conclusive evidence that the population of this level proceeds via a single-step direct transition.

Two other states of ^{26}Mg at $E_x=9.111$ and 9.383 MeV are also assigned $J^\pi=6^+$ in Ref. [21], but they are weakly populated, if at all, in the present work.

E. Comparison between experimental and shell-model excitation energies and spectroscopic factors for positive-parity states

Excitation energies and one-proton pickup spectroscopic factors have been calculated in the framework of the shell model for the ^{26}Mg levels which are populated through the $2s_{1/2}$, $1d_{3/2}$, and $1d_{5/2}$ transitions. As expected from the position of the ^{27}Al nucleus in the shell, most of the strength is carried out by the $1d_{5/2}$ transi-

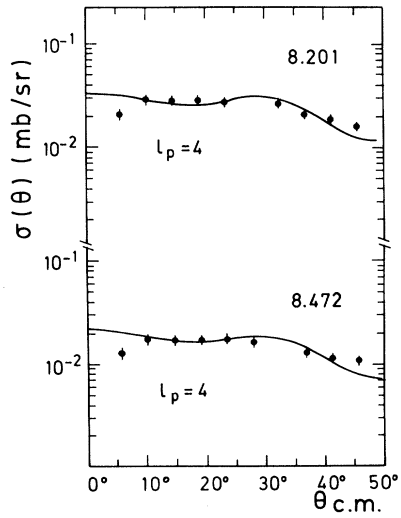

FIG. 8. Angular distributions from the ^{27}Al(d,^{3}He)^{26}Mg reaction leading to the levels at $E_x=8.201$ and 8.472 MeV, $J^\pi=6^+$. The curves are from a DWBA calculation done with the assumption of a $l_p=4$, $1g_{9/2}$ transition.

tions since the total spectroscopic strength $\sum C^2S$ which is calculated for *all* the positive-parity states with $J^\pi \leq 5^+$ amounts to 4.108, 0.421, and 0.470 for the $1d_{5/2}$, $2s_{1/2}$, and $1d_{3/2}$ transitions, respectively. The results of the calculations are presented in Table V for the first eight levels with $0^+ \leq J^\pi \leq 5^+$. The excitation energies are presented in column 1 and the spectroscopic factors in columns 5, 6, and 7. It is observed that the percentage of the total predicted spectroscopic strength which is carried out by the levels of Table V amounts to about 90% for the levels

TABLE V. Comparison of experimental excitation energies, J^π values, and spectroscopic factors in ^{26}Mg with the predictions of shell-model calculations.

Excitation energies and J^π values				Spectroscopic factors S					
Shell model		(a)		Shell model				This work	
E_x (MeV)	J_i^π	E_x (MeV)	J^π	$2s_{1/2}$	$1d_{3/2}$	$1d_{5/2}$	$l_p=2$	$l_p=2$	$l_p=0$
0.000	0_1^+	0.000	0^+			0.418	0.42	0.46	
1.929	2_1^+	1.809	2^+	0.020	0.001	1.287	1.29	1.50	0.009
3.153	2_2^+	2.938	2^+	0.032	0.040	0.159	0.19	0.33	0.023
3.681	0_2^+	3.589	0^+			0.005	<0.01	0.009	
3.921	3_1^+	3.941	3^+	0.012	0.031	0.001	0.03	0.030	0.008
4.511	3_2^+	4.350	3^+	0.098	0.043	0.007	0.05	0.17	0.090
4.533	4_1^+	4.318	4^+		0.043	2.485	2.51	2.93	
4.541	2_3^+	4.332	2^+	0.045	0.008	0.093	0.10		0.036
4.932	4_2^+	4.900	4^+		0.000	0.002	<0.01	(0.024)	
5.000	2_4^+	4.834	2^+	0.240	0.059	0.064	0.10	0.12	0.14
5.204	0_3^+	4.972	0^+			0.002	<0.01	0.003	
5.404	2_5^+	5.291	2^+	0.001	0.008	0.009	0.02	0.017	0.024
5.473	4_3^+	5.474	4^+		0.000	0.296	0.30	0.31	
5.833	1_1^+	5.690	1^+		0.003	0.028	0.03	0.045	
6.009	4_4^+	5.716	4^+		0.051	0.009	0.06	0.11	
6.062	0_4^+	6.256	0^+			0.000	0.00		
6.268	3_3^+	6.125	3^+	0.038	0.055	0.003	0.06	0.11	0.039
6.647	2_6^+	(6.634)	$(0-4)^+$	0.000	0.002	0.065	0.07	0.044	
6.777	4_5^+	6.622	4^+		0.003	0.001	<0.01		
6.798	1_2^+				0.004	0.007	0.01		
6.843	2_7^+	(6.745)	2^+	0.000	0.000	0.033	0.03	0.020	<0.002
7.038	5_1^+	6.978	5^+			0.000	0.00	0.057	
7.093	2_8^+	7.100	2^+	0.002	0.027	0.042	0.06	0.09	
7.282	3_4^+	7.242	$(2,3)^+$	0.065	0.047	0.109	0.14	0.14	0.035
7.411	4_6^+	7.677	$(3,4)^+$		0.017	0.060	0.07	0.10	
7.465	5_2^+	7.395	5^+			0.123	0.12	0.13	
7.602	3_5^+			0.000	0.000	0.002	<0.01		
7.721	1_3^+				0.004	0.009	0.01		
7.941	4_7^+	(7.724)	$(2-5)^+$		0.002	0.025	0.03	0.072	
8.005	3_6^+	(7.773)	$(2-4)^+$	0.002	0.006	0.047	0.05	(0.038)	
8.131	0_5^+					0.000	0.00		
8.404	3_7^+			0.010	0.022	0.051	0.07		
8.413	4_8^+	(8.703)	$(2-4)^+$		0.024	0.112	0.13	0.18	
8.443	1_4^+				0.004	0.012	0.01		
8.520	5_3^+					0.000	0.00		
8.645	0_6^+					0.000	0.00		
8.935	5_4^+	9.064	5^+			0.048	0.05	(0.075)	
9.081	1_5^+				0.001	0.000	<0.01		
9.115	3_8^+			0.001	0.033	0.006	0.04		
9.146	1_6^+				0.001	0.000	<0.01		
9.458	5_5^+					0.005	0.01		
9.643	1_7^+				0.000	0.000	0.00		
9.768	5_6^+					0.000	0.00		
9.827	1_8^+				0.000	0.003	<0.01		
10.079	0_7^+					0.000	0.00		
10.255	5_7^+					0.001	<0.01		
10.333	0_8^+					0.000	0.00		
10.505	5_8^+					0.012	0.01		

[a]Reference [4] and this work. The levels which are presented in parentheses can also be identified with one or several other shell-model states (see text, Sec. V E).

involving the configurations $2s_{1/2}$ and $1d_{5/2}$ (with about 70% of the $1d_{5/2}$ strength upon the levels with $J^\pi=0_1^+$, 2_1^+, and 4_1^+) and to about 75% only for those which involve configuration $1d_{3/2}$. It is also observed that spectroscopic factor values larger than 0.05 are predicted for a number of levels with excitation energies higher than 6 MeV. Such spectroscopic factor values should lead to prominent enough peaks in the experimental spectra so that it is an incitement to attempt the identification of experimental levels with shell-model predicted levels in the whole excitation energy range of the present work.

As indicated in Sec. IV, the $J^\pi=(1-4)^+$ levels can be populated through $1d_{5/2}$ and $1d_{3/2}$ transitions with the same DWBA shapes. The shell-model spectroscopic factor values of the $l_p=2$ transitions leading to these levels were calculated by taking into account that the cross section is the incoherent sum of a $1d_{3/2}$ and a $1d_{5/2}$ contribution and can be written as

$$S_{l_p=2}\left[\frac{d\sigma_{l_p=2}(\theta)}{d\omega}\right]_{\text{DWBA}}=\left\{\frac{S(d_{3/2})}{4}\left[\frac{d\sigma_{d_{3/2}}(\theta)}{d\omega}\right]_{\text{DWUCK4}}+\frac{S(d_{5/2})}{6}\left[\frac{d\sigma_{d_{5/2}}(\theta)}{d\omega}\right]_{\text{DWUCK4}}\right\}. \tag{4}$$

So, by introducing into the relationship (4) the value of 2.17, which is the ratio of the DWUCK4 cross sections for the $1d_{5/2}$ and $1d_{3/2}$ transfers (see Sec. IV), the values of column 8 are obtained from the values of columns 6 and 7 through the relationships

$$S_{l_p=2}=S_{\text{SM}}(d_{5/2})+0.69S_{\text{SM}}(d_{3/2}) \tag{5}$$

if the experimental angular distribution is analyzed with the assumption of a transfer $1d_{5/2}$ and

$$S_{l_p=2}=S_{\text{SM}}(d_{3/2})+1.45S_{\text{SM}}(d_{5/2}) \tag{6}$$

with the other assumption. The shell-model predicted dominant transfer was adopted to get the $S_{l_p=2}$ values.

There is no problem for establishing a correspondence between the experimental and shell-model levels up to the experimental level at $E_x=6.125$ MeV (Table V and Fig. 9). The mean value of the deviation between the experimental and shell-model excitation energies of the first 16 excited levels is about 150 keV, and the largest deviation (slightly less than 300 keV) is observed for the 5.716–6.009 MeV pair, $J^\pi=4_4^+$. Experimental and shell-model spectroscopic factors generally agree to substantially better than a factor of 2 with the exception of the levels at $E_x=4.350$, 4.900, and 5.291 MeV, which will be considered later. In the case of the levels with $J^\pi=(2,3)^+$, the values which are obtained for the weight α of the $l_p=0$ transition in the mixed $l_p=0+2$ transitions (Sec. IV) are compared in Table VI with the values which can be easily deduced from the shell-model spectroscopic factors of Table V. Except for the two levels at $E_x=4.350$ and 5.291 MeV, there is a correct agreement within a factor of 2, or better, between the experimental and shell-model predicted values of α, but the shell-model values are larger than the experimental ones in almost all cases. This agreement brings some *a posteriori* support to the method which was used to get the weight α from the experimental data despite the sources of imprecision as discussed in Sec. IV. Most of the experimental spectroscopic factor values for the $l_p=2$ transitions are larger than the shell-model predicted ones, even for the pure $l_p=2$ transitions. On the other hand, more $l_p=0$ strength is predicted by the shell-model calculations than measured in the experiment, but this can be due mostly

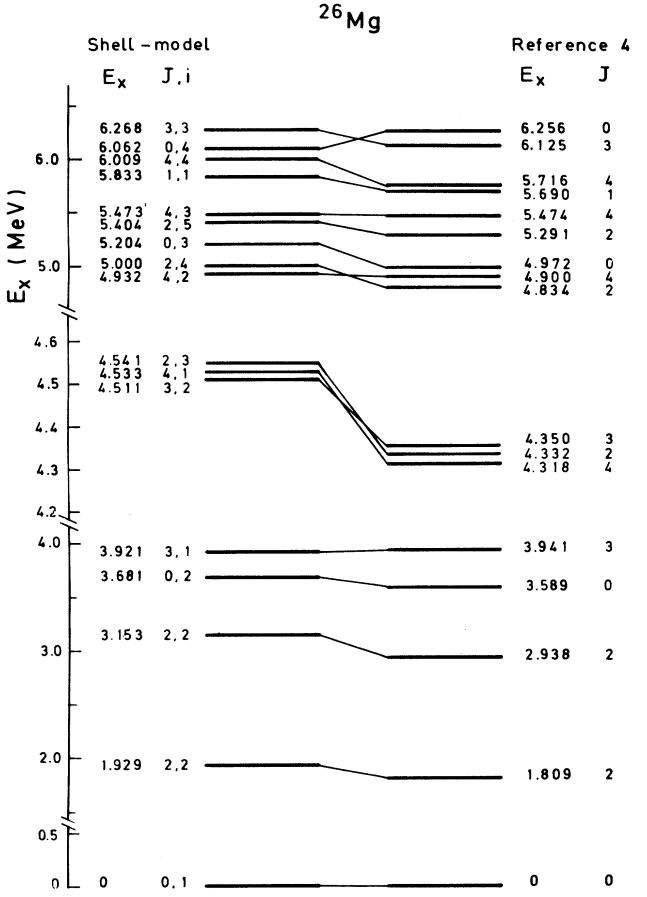

FIG. 9. Identification of experimental positive parity levels in ^{26}Mg with shell-model predicted levels in the $0\leq E_x\leq 6.5$ MeV excitation energy range. This identification is done as explained in text (Sec. V E). The ith shell-model level with spin J is presented in the column "J,i." As to the experimental levels, the excitation energies are from Ref. [4] and the J^π values are from Ref. [4] or from the present work (Table I). In order to make the visual comparison more evident, the triplet of levels around $E_x\sim 4.5$ MeV is presented with an expanded excitation energy scale. The level at $E_x=6.256$ MeV, $J^\pi=0^+$, is not observed in this work. However, it is identified with the shell-model level at $E_x=6.062$ MeV, $J^\pi=0_4^+$, because the predicted spectroscopic factor is $S=0.00$ (Table V).

TABLE VI. Percentage of the $l_p=0$ contribution in the $l_p=0+2$ transitions.

Shell model			a		
E_x (MeV)	J_i^π	α	E_x (MeV)	J_i^π	α^b
1.929	2_1^+	0.02	1.809	2^+	0.01
3.153	2_2^+	0.15	2.938	2^+	0.07
4.541	2_3^+	0.31	4.332	2^+	
5.000	2_4^+	0.70	4.834	2^+	0.53
5.404	2_5^+	0.06	5.291	2^+	0.60
6.647	2_6^+	0.00			
6.843	2_7^+	0.00	(6.745)	2^+	0.08
7.093	2_8^+	0.03	7.100	2^+	0.00
3.921	3_1^+	0.27	3.941	3^+	0.22
4.511	3_2^+	0.65	4.350	3^+	0.31
6.268	3_3^+	0.39	6.125	3^+	0.23
7.282	3_4^+	0.32	7.242	$(2,3)^+$ [b]	0.20
7.602	3_5^+	0.00			
8.005	3_6^+	0.04			
8.404	3_7^+	0.13			
9.115	3_8^+	0.02			

[a]The excitation energies and J^π values are from Ref. [4] unless indicated.
[b]This work.

to the smaller experimental values of α.

Despite the care which was brought to the analysis of the spectra with the code PICOTO, the peak corresponding to the level at $E_x=4.350$ MeV could contain a contribution from the much more intense peak corresponding to the levels at $E_x=4.318$ and 4.332 MeV and this contribution would thus be responsible of the experimental excess of $l_p=2$ strength in the level at $E_x=4.350$ MeV. The experimental angular distribution of the transition to $E_x=4.900$ MeV is accounted for poorly by the DWUCK4 calculations (Fig. 4). So the experimental spectroscopic factor value can be of no significance. As to the level at $E_x=5.291$ MeV, the important contribution of the $l_p=0$ transition, which is clearly apparent from the pattern of the experimental angular distribution (Fig. 5), is not predicted by the shell-model calculations.

The success of this identification for the levels with $E_x\leq 6.125$ MeV is an incitement to attempt a similar identification for levels at higher excitation energies. However, it is felt that this identification is made less evident first because the density of the experimental and shell-model levels is increasing and second because the incertitude due to the DWBA analysis is expected to be larger for the experimental spectroscopic factors of these weakly enough populated levels. Furthermore, it has been pointed out in Sec. IV that there was a degradation of the DWBA fit to the experimental angular distributions for the $l_p=2$ transitions at higher excitation energies. Anyway, the identification was attempted as for the lower levels on the grounds of the agreement between the experimental and shell-model spectroscopic factors (within a factor of 2) and excitation energies (within ± 300 keV). This identification is presented in Table V and Fig. 10. The levels at $E_x=6.622$, 6.978, 7.100, 7.395, and 9.064 MeV ($J^\pi=4^+$, 5^+, 2^+, 5^+, and $J=5$, respectively) can thus be reasonably identified with the shell-model levels at $E_x=6.777$, 7.038, 7.093, 7.465, and 8.935 MeV with $J^\pi=4_5^+$, 5_1^+, 2_8^+, 5_2^+, and 5_4^+, respectively, despite the fact that no pickup strength is predicted for the 5_1^+ level in the shell-model calculations. Similarly, the levels at $E_x=7.242$ and 7.677 MeV, $J^\pi=(2,3)^+$ and $(3,4)^+$, respectively, can be identified with the shell-model levels at $E_x=7.282$ and 7.411 MeV with $J^\pi=3_4^+$ and 4_6^+, respectively. Another argument for the identification of the level at $E_x=7.677$ MeV with the $J^\pi=4_6^+$ level could come from a study of the one-neutron stripping reaction on ^{25}Mg since this level is predicted by shell-model calculations to be strongly populated ($S_n=0.24$) in this reaction. An intense peak which is attributed to the excitation of the two unresolved levels at $E_x=7.677+7.694$ MeV was indeed observed in a study of the ^{25}Mg$(d,p)^{26}$Mg reaction [20]. However, the analysis of the experimental angular distribution which should display (if the two levels were populated) a pattern due to the superposition of $l_n=1$ and 2 transitions has not been done.

The levels at $E_x=6.634$ and 6.745 MeV, $J^\pi=(0-4)^+$ and 2^+, respectively, are tentatively identified with the shell-model levels at $E_x=6.647$ and 6.843 MeV, $J^\pi=2_6^+$ and 2_7^+, respectively. This identification is only tentative because the inverted identification seems to be as likely as this one. For this reason the two levels at $E_x=6.647$ and 6.745 MeV are presented in parentheses in Table V. Anyway, it would lead to the $J^\pi=2^+$ assignment to the level at $E_x=6.634$ MeV.

Furthermore, as the excitation energy is increasing, a supplementary difficulty for identifying the levels comes from the fact that the shell-model calculations are restricted to the first eight levels with $0^+\leq J^\pi\leq 5^+$. The levels with $J^\pi=2_8^+$, 3_8^+, and 4_8^+ are predicted to lie at $E_x=7.093$, 9.115, and 8.413 MeV, respectively, whereas experimental levels are indeed observed in this work up to about 9.7 MeV. The lack of knowledge about the

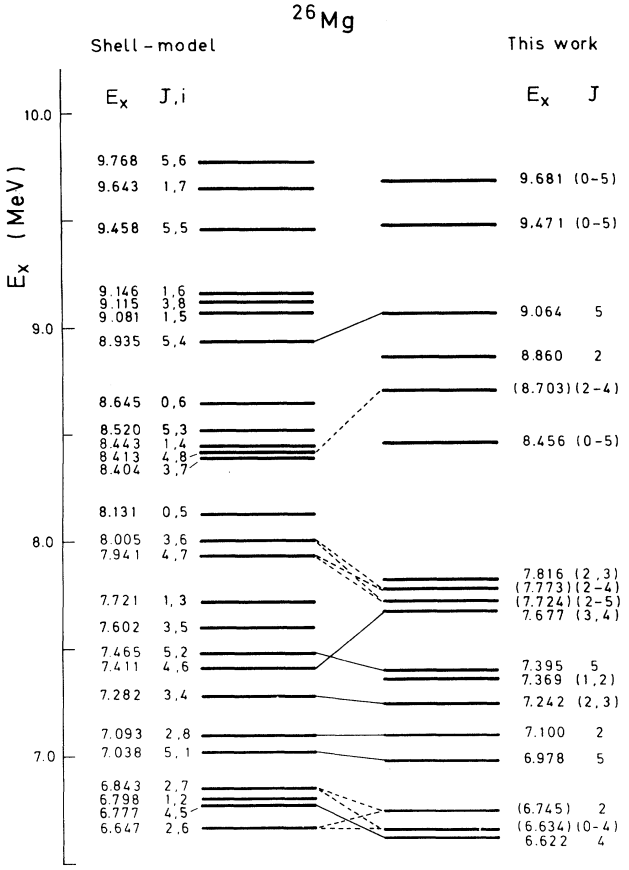

FIG. 10. Identification of experimental positive-parity levels in ^{26}Mg with shell-model predicted levels in the $6.5 \leq E_x \leq 9.8$ MeV excitation energy range. This identification is done as explained in text (Sec. V E). The ith shell-model level with spin J is presented in the column "J,i." Only the experimental levels which are observed in this work (Table I) are presented in this figure. Their excitation energies are from Ref. [4], and the J^π values are from Ref. [4] or from the present work (Table I). The dashed line which connects experimental and shell-model levels means that the identification is only tentative in this case (see text, Sec. V E).

shell-model levels with $J^\pi = 2_i^+$, 3_i^+, and 4_i^+ with $i > 8$ can make the identification not completely sure since it has been pointed out above that the total spectroscopic strength is not completely exhausted by the first eight shell-model levels (especially for the $1d_{3/2}$ transition). It is the case, for instance, for the level at $E_x = 8.703$ MeV, $J^\pi = (2-4)^+$. The identification of this level with the shell-model level at $E_x = 8.404$ MeV, $J^\pi = 3_7^+$, seems unlikely because no measurable $l_p = 0$ strength could be evidenced from the experimental data, whereas a weight $\alpha = 0.13$ is predicted by the shell-model calculations (Table VI). On the other hand, the identification with the level at $E_x = 8.413$ MeV, $J^\pi = 4_8^+$, seems reasonable, but it cannot be considered as completely firm since nothing is known about the energies and spectroscopic factors of the shell-model levels with $J^\pi = 2_{i>8}^+$. It is also the case for the levels at $E_x = 7.724$ and 7.773 MeV, $J^\pi = (2-5)^+$ and $(2-4)^+$, respectively, which are tentatively identified with the shell-model levels at $E_x = 7.941$ and 8.005 MeV, $J^\pi = 4_7^+$ and 3_6^+, respectively (though in this case also the inverted identification may be considered as likely as this one). However these levels can also correspond to up to now unknown $J^\pi = 2^+$ shell-model levels. All these levels for which the identification is considered as not firm are presented in parentheses in Tables V and VI. The lack of knowledge of the shell-model levels with $J^\pi = 2_i^+$, 3_i^+, and 4_i^+ with $i > 8$ prevented also any attempt of identification of the experimental levels at $E_x = 7.369$, 7.816, 8.456, 8.860, 9.471, and 9.681 MeV.

VI. SUMMARY

The present study provides an accurate determination of the excitation energy of the two intense fragments which were attributed in Ref. [2] to the population of hole states in the $1p_{1/2}$ subshell. Furthermore, it yields some evidence for the presence of a contribution of the g shell (and may be of the p and f shells) in the ground state of ^{27}Al. At last, the agreement between the experimental and shell-model predicted spectroscopic factors and excitation energies is such as the use of the identification of an experimental-shell-model pair as a spectroscopic tool for the J^π assignment to the experimental member can be reasonably considered in some cases.

ACKNOWLEDGMENTS

The authors are indebted to J. Izac for the aluminum target preparation. They acknowledge the operating crew of the Orsay MP Tandem for the efficient running of the accelerator. This work was supported in part by the U.S. National Science Foundation.

[1] B. H. Wildenthal and E. Newman, Phys. Rev. **175**, 1431 (1968).
[2] G. J. Wagner, G. Mairle, U. Schmidt-Rohr, and P. Turek, Nucl. Phys. **A125**, 80 (1969).
[3] M. Arditi, L. Bimbot, H. Doubre, N. Frascaria, J. P. Garron, M. Riou, and D. Royer, Nucl. Phys. **A165**, 129 (1971).
[4] P. M. Endt, Nucl. Phys. **A521**, 1 (1990).
[5] L. Lapikás and P. K. A. de Witt Huberts, J. Phys. (Paris) Colloq. **C4**, 57 (1984).
[6] W. W. Daehnick, J. D. Childs, and Z. Vrcelj, Phys. Rev. C **21**, 2253 (1980).
[7] J. Vernotte, A. Khendriche, G. Berrier-Ronsin, S. Grafeuille, J. Kalifa, G. Rotbard, R. Tamisier, and B. H. Wildenthal, Phys. Rev. C **41**, 1956 (1990).
[8] P. Picot, Internal Report of Institut de Physique Nucléaire Orsay No. IPNO-T-81-03, Orsay, 1981.
[9] J. R. Comfort, Argonne National Laboratory Physics Division Informal Report No. Phy-1970 B, 1970 (unpub-

lished).
[10] P. D. Kunz (private communication).
[11] R. H. Bassel, Phys. Rev. **149**, 791 (1966).
[12] E. Newman, L. C. Becker, B. M. Preedom, and J. C. Hiebert, Nucl. Phys. **A100**, 225 (1967).
[13] G. Mairle, K. T. Knöpfle, H. Riedesel, G. J. Wagner, V. Bechtold, and L. Friedrich, Nucl. Phys. **A339**, 61 (1980).
[14] F. Hinterberger, G. Mairle, U. Schmidt-Rohr, G. J. Wagner, and P. Turek, Nucl. Phys. **A111**, 265 (1968).
[15] H. Mackh, G. Mairle, and G. J. Wagner, Z. Phys. **269**, 353 (1974).
[16] J. Vernotte, G. Berrier-Ronsin, J. Kalifa, and R. Tamisier, Nucl. Phys. **A390**, 285 (1982).
[17] W. P. Alford, J. A. Cameron, E. Habib, and B. H. Wildenthal, Nucl. Phys. **A454**, 189 (1986).
[18] U. E. P. Berg, K. Ackermann, K. Bangert, C. Bläsing, W. Naatz, R. Stock, and K. Wienhard, Phys. Lett. **140B**, 191 (1984).
[19] G. M. Crawley, C. Djalali, N. Marty, M. Morlet, A. Willis, N. Anantaraman, B. A. Brown, and A. Galonsky, Phys. Rev. C **39**, 311 (1989).
[20] H. F. R. Arciszewski, E. A. Bakkum, C. P. M. van Engelen, P. M. Endt, and R. Kamermans, Nucl. Phys. **A430**, 234 (1984).
[21] F. Glatz, S. Norbert, E. Bitterwolf, A. Burkard, F. Heidinger, Th. Kern, R. Lehmann, H. Röpke, J. Siefert, C. Schneider, and B. H. Wildenthal, Z. Phys. A **324**, 187 (1986).
[22] B. H. Wildenthal and E. Newman, Phys. Rev. **167**, 1027 (1968).
[23] H. E. Gove, K. H. Purser, J. J. Schwartz, W. P. Alford, and D. Cline, Nucl. Phys. **A116**, 369 (1968).